International Journal of Innovative Research and Scientific Studies, 8(9) 2025, pages: 326-341

IJIRSS
International Journal of Innovative Research & Scientific Studies

ISSN: 2617-6548

URL: www.ijirss.com

Formulating a semi-empirical equation for the shearing modulus of rigid pavement slabs

Tjatur Haripriambodo[1*], Sofia W. Alisjahbana[2], Najid[3], Jack Widjajakusuma[4]

[1,3]*Civil Engineering Doctoral Program, Universitas Tarumanagara, Grogol Petamburan, Jakarta Barat, 11440, Indonesia.*
[2]*Bakrie University, Kuningan, Jakarta Selatan, 12940, Indonesia.*
[4]*Universitas Pelita Harapan, Lippo Karawaci, Tangerang, 11000, Indonesia.*

Corresponding author: Tjatur Haripriambodo (*Email: tjatur264@gmail.com*)

Abstract

A rigid pavement consists of a subbase, base, and a surface in the form of concrete slabs with varying thicknesses and strengths. The design methods currently known are the AAHSTO, PCI, ACI, and others, which are traditionally based on analytical solutions of beams or long plates supported by an elastic foundation under static loads. Recently, research has emphasized dynamic modeling and analysis of loads. Other research focused on a parametric study to identify key aspects of the dynamic behavior of rigid pavement slabs on an elastic layer. The Pasternak model presented a spring layer and a shearing layer to simulate the dynamic behavior of the slab. A shearing layer contributes to dynamic behavior through the shearing modulus (G_{max}), where it plays a role in dynamic analysis. This research is purposed at formulating the empirical equation for the shear modulus of the subbase layer of toll road rigid pavement in Indonesia based on soil samples taken from beneath the rigid pavement. The result of this research shows that G_{max} values (unit MPa) based on Kakusho equations are 24.294 (max) and 16.325 (min), Marcuson's are 32.015 (max) and 22.306 (min), Menard's are 34.527 (max) and 10.634 (min). All G_{max} tend to be within similar corridors. While Hardin's are 67.112 (max) and 31.982 (min), it tends to be higher than other G_{max} values above. Other result was a semi-empirical equation successfully developed to calculate G_{max} from plasticity index (Ip) : $G_{max} = 0.0313(Ip)^2 - 3.1147Ip + 88.798$. By having those results, designing a rigid pavement slab may be used above G_{max} values and equations to carry a dynamic analysis design.

Keywords: Rigid pavement slab, Shear modulus, Shearing modulus.

DOI: 10.53894/ijirss.v8i9.10694
Funding: This study received no specific financial support.
History: Received: 12 August 2025 / **Revised:** 15 September 2025 / **Accepted:** 17 September 2025 / **Published:** 20 October 2025

Competing Interests: The authors declare that they have no competing interests.
Authors' Contributions: All authors contributed equally to the conception and design of the study. All authors have read and agreed to the published version of the manuscript.
Transparency: The authors confirm that the manuscript is an honest, accurate, and transparent account of the study; that no vital features of the study have been omitted; and that any discrepancies from the study as planned have been explained. This study followed all ethical practices during writing.
Publisher: Innovative Research Publishing

1. Introduction

The addition of toll road length in Indonesia has been very rapid in recent years. According to data from the Toll Road Regulatory Agency (BPJT) of the Ministry of Public Works of the Republic of Indonesia, in 2025 toll roads will operate with a total length of 3,020 km, consisting of 75 toll road sections. Toll roads generally use rigid pavement/concrete. Rigid pavement consists of a subbase layer, base layer, and a surface in the form of concrete slabs with varying thicknesses and concrete strengths.

The rigid pavement design methods currently known are the AAHSTO, PCI, ACI, and others, which are traditionally based on analytical solutions of beams or long plates supported by an elastic foundation under static loads [1]. At present, rigid pavement design models moving loads as static loads, even though they actually have dynamic characteristics [2]. Sawant (2010) stated, "the most available analytical solutions represent the pavement by an infinitely long beam or plate and neglect dynamic interaction between the moving load and pavement" [3].

Subsequent developments in research on moving loads modeled/analyzed dynamically have continued to progress. In 2003, Alisjahbana and Wangsadinata studied the dynamic response of rigid pavement to dynamic loads. The rigid pavement slab was modeled as a square, orthotropic plate supported by an elastic foundation [4]. In 2004, Rahman and Anam conducted a parametric study to identify important aspects of the dynamic behavior of rigid pavement slabs on an elastic layer. The modeling used was Winkler foundation, Pasternak foundation, and Vlasov foundation [5]. In 2016, Nguyen et al. used Winkler and Pasternak modeling to obtain an overview of the dynamic response of a beam subjected to dynamic loads [6].

Subsequent research began using modeling that was a development of the Winkler foundation model, namely the Pasternak model and the Kerr model. In 2018, Alisjahbana et al. proposed a semi-analytical solution for the plate problem with Kerr modeling due to moving loads [7]. The main difference between the Winkler, Pasternak, and Kerr models lies in the shearing layer, which is only present in the Pasternak and Kerr models.

This research is aimed at formulating the equation for the shear modulus of the subbase layer of rigid toll road pavement in Indonesia based on soil samples taken from beneath the rigid pavement, which will then be tested in the laboratory. The results obtained are useful for the dynamic analysis of concrete slabs/rigid pavement subjected to dynamic loads in the form of moving vehicle loads.

1.1. Plates on Elastic Foundation

In 1954, Pasternak developed the Winkler model by adding a shearing layer located between the plate and the spring layer. In 1964, A. D. Kerr proposed a development of the previous model by adding a spring layer, so that the Kerr model consists of two spring layers and one shearing layer [8].

In general, the modeling of beams or plates on an elastic foundation satisfies the equilibrium conditions (see Figure 1).

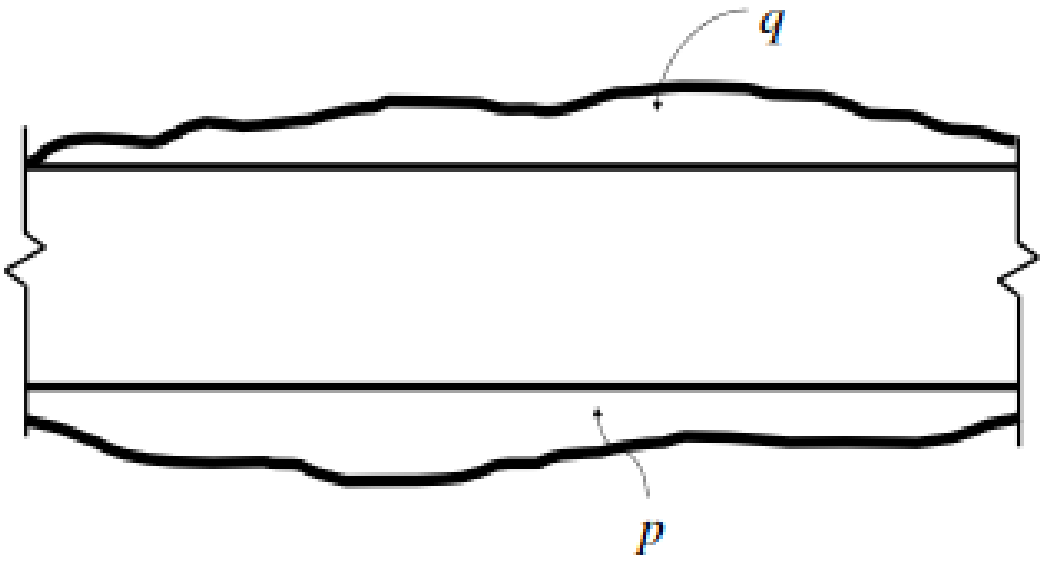

Figure 1.
Beam on equilibrium condition Das [8].

$$EI\frac{\partial^4 w}{\partial x^4} = q - p \qquad (1)$$

E is the modulus of elasticity of the plate/beam, I is the moment of inertia of the beam/plate, w is the vertical deflection experienced by the plate, while q is the load acting on the plate including self-weight, and p is the response of the foundation.

1.2. Pasternak Model

The Pasternak model is the first model to place a shearing layer in the modeling of a plate on an elastic foundation. The shearing layer is located beneath the plate and above the spring layer. A one-dimensional beam with Pasternak modeling is presented in Figure 2 below.

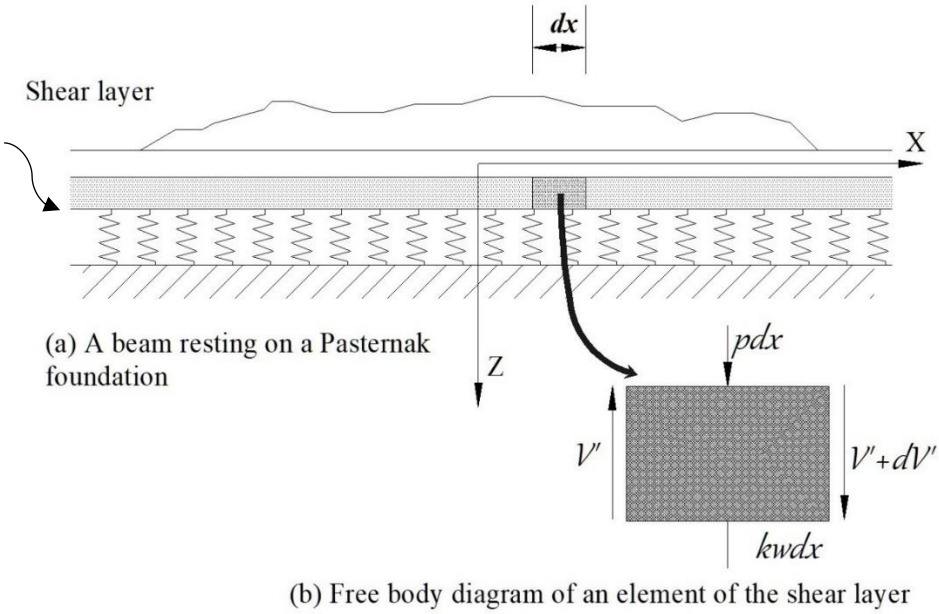

Figure 2.
Free-body diagram of the shearing layer element Das [8].

Governing equation for Pasternak one-dimensional beam is as follows (Equation 2).

$$EI\frac{\partial^4 w}{\partial x^4} - G_s\frac{\partial^2 w}{\partial x^2} + kw = q \qquad (2)$$

G_s is the shear modulus, which is an indication of the shearing layer parameter, and k is the coefficient of the spring layer. It is clearly seen that the Pasternak model is a modeling approach that incorporates a shearing layer.

2. Literature Review

Research on shear modulus has been widely conducted by researchers for various purposes. One important study was carried out by Hardin and Drnevich [9] to obtain equations and curves for shear modulus and damping modulus [9]. A few years later Iwasaki, et al. [10] and colleagues conducted a study on the shear modulus equation of sandy soil using cyclic torsional loading Iwasaki, et al. [10]. Gabryś and Szymański [11] researched the shear modulus of cohesive soil Gabryś and Szymański [11]. Nasarani, et al. [12] studied the effect of adding volcanic ash on the maximum shear modulus through triaxial testing [12]. Similarly, Purwanto [13] conducted research on shear modulus based on the equations of Purwanto [13]. Another study in 2015 by Massarsch involved determining the shear modulus from static and seismic penetration tests [14]. Research correlated with shear modulus, namely the study of the Overconsolidated Ratio (OCR) of clay soil, was conducted by Mayne [15].

Another significant research conducted by Wong, et al. [16]. This research emphasized an extended model of the shear modulus reduction in cohesive soil. According to this research, there was a degradation in hyperbolic curve relationship with increasing shear strain. In Zsolt Szilvágyi1, et al. [17] determined soil shearing modulus from the resonant column, the torsional shear and bender element tests. This research showed that shear modulus value from resonant column was like torsional test value [17]. The newest research was established a mathematical model for the estimation of shear modulus for unsaturated compacted soils, conducted by Zhai, et al. [18]. In this research, a new mathematical model was proposed for the estimation of the shear modulus function.

3. Research Method

This research is a combination of utilizing primary data in the form of in-situ soil samples (undisturbed soil sample, UDS) and the implementation of empirical equations obtained from previous studies. In general, the research flow is shown in Figure 3.

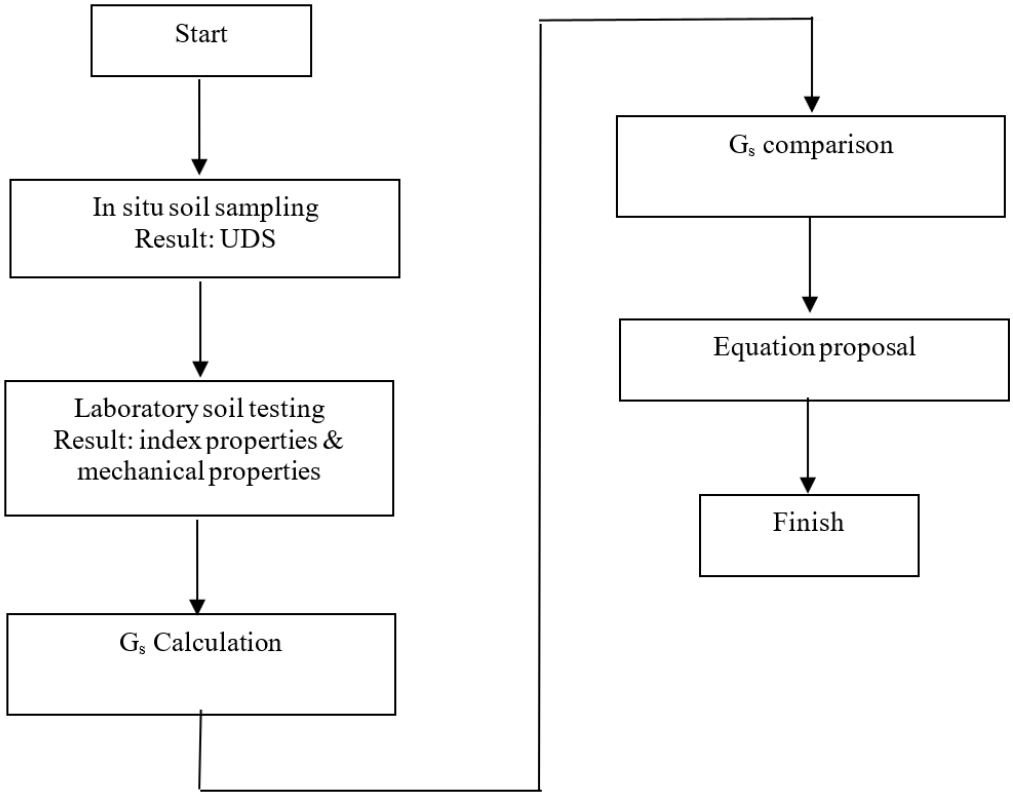

Figure 3.
Research flow.

3.1. Shearing Modulus

The parameter that indicates the condition of the shearing layer is the shear modulus. The shear modulus of soil (G_s) is the ratio between shear stress (S_s) and shear strain (ε_s). The shear modulus has a relationship with the modulus of elasticity (Young's modulus, E_s) and Poisson's ratio. The shear modulus equation is presented as follows (Equation 3) [19].

$$G'_s = \frac{S_s}{\epsilon_s} = \frac{E_s}{2(1+\mu)} \quad (3)$$

The shear modulus (G_s) is a soil parameter that plays a role in dynamic analysis [11]. Thus, the influence of the shear modulus is very significant on the dynamic analysis of rigid pavement slabs.

Currently, there are several empirical equations for calculating the maximum shear modulus (G_{max}). These various equations require verification to determine whether they are in accordance with the available deformation parameters [11]. Several well-known equations are presented in Table 1.

Table 1.
Maximum shear modulus equation.

1	$G_{max} = \frac{445.(4.4-e)^2}{1+e}(\sigma'_0)^{0.5}$	Marcuson and Wahls [20]	Cohesive clayey
2	$G_{max} = \frac{90.(7.32-e)^2}{1+e}(\sigma'_0)^{0.6}$	Kakusho and Yanagida [21]	Cohesive clayey
3	$G_{max} = \frac{1230.(2.973-e)^2 OCR^k}{1+e}\sqrt{\sigma'_0}$	Hardin and Drnevich [9]	Cohesive and sand
4	$G_{max} = \frac{E}{2(1+\nu)R_M}$	Menard [22]	

Note: e : void ratio;
OCR : overconsolidated ratio;
σ'_0 : mean effective principal stress
In the equation above, G_{max} has units of Psi.

For Equation 3 in Table 1, there is a coefficient k determined based on the Plasticity Index (Ip) parameter. The value of k is determined based on the Ip value shown in Table 2.

Table 2.
k value according to Ip.

I_P (%)	**20**	**40**	**60**	**80**	**≥ 100**
k	0.18	0.30	0.41	0.48	0.50

In Equation 4 in Table 1, the parameters required are the soil modulus of elasticity (E), the soil Poisson's ratio, and the R_M coefficient, which is a function of the Plasticity Index (I_p). R_M is calculated by implementing Equation 4 below.

$$R_{\mathrm{M}} = 0.0043\mathrm{Ip} + 0.103 \quad (4)$$

3.2. Calculation of the Parameters Involved

Referring to the *Standard Test Method for CU Triaxial Compression Test for Cohesive Soil* (ASTM D4767 – 11) Reapproved 2020 [14], the mean effective principal stress, σ_0', is calculated using Equation 5 as presented below.

$$\sigma'_0 = \frac{\sigma_1 + \sigma_3}{2} \quad (5)$$

s_1 : major principal stress from the Triaxial test

s_3 : minor principal stress from the Triaxial test

The Overconsolidated Ratio (OCR) is the ratio between the preconsolidation pressure (before natural consolidation) and the effective overburden stress [15]. In-situ investigation of OCR is not easy to carry out due to the sample disturbance effect in natural soil samples. An alternative for determining OCR is through laboratory testing, particularly triaxial (undrained) and direct shear tests. The following is Equation (6) for calculating OCR based on triaxial test results.

$$OCR = \left[\frac{\left(C_u/\sigma'_{v0}\right)}{0.75sin\emptyset'}\right]^{1/\Lambda} \quad (6)$$

Equation 7 refers to Skempton (1954/1957), in the journal *"Overconsolidation Ratio Determination of Cohesive Soil"* by Urbaitis, et al. [23]

$$\frac{C_u}{\sigma'_{v0}} = 0.11 + 0.371\mathrm{I_p} \quad (7)$$

I_P : plasticity index (%), obtained from the Atterberg limits test. f is an internal shearing angle which obtained from Triaxial test. The last coefficient is Λ which took 0.7 as the value as suggested by Urbaitis, et al. [23].

Equation 4 in Table 1, consists of poisson ratio (n) and elastic modulus (E). Poisson ratio took value as listed in Table 3. While E implemented values from Triaxial test.

Table 3.
Poisson's ratio (n) values for several types of soil [19].

Soil type	**n**
Clay, saturated	0.4 – 0.5
Clay, unsaturated	0.1 – 0.3
Sandy clay	0.2 – 0.3
Silt	0.3 – 0.35
Sand, gravelly sand	0.1 – 1.00
Most common	0.3 – 0.4
Rock	0.1 – 0.4

3.3. Soil Sampling

The location of field study was in Cikampek – Palimanan (Cipali) toll road which part of trans Java toll road. Cipali toll road stretches from Cikampek (Karawang regency) to Palimanan (Cirebon regency). Total length of Cipali toll road is 116 kms. The original pavement type of Cipali Toll Road is concrete (rigid) pavement. Nonetheless some locations have been overlayed by asphalt. The definite location where field study was conducted was in Sta. 178 Jakarta direction. In this location, the pavement is concrete (rigid) with layers as shown in Figure 4.

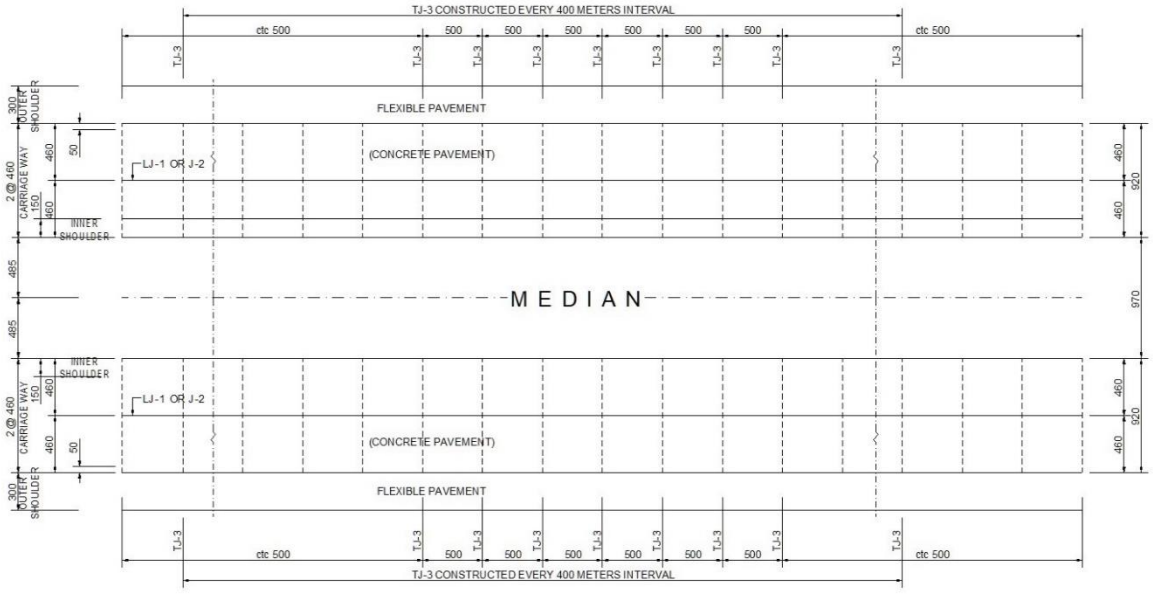

Figure **4.**
Pavement plan.

Original design of Cipali toll road is two lanes for each direction. Typical dimension slab is 5.0 x 4.0 m. Comprehend cross section is presented in Figure 4.

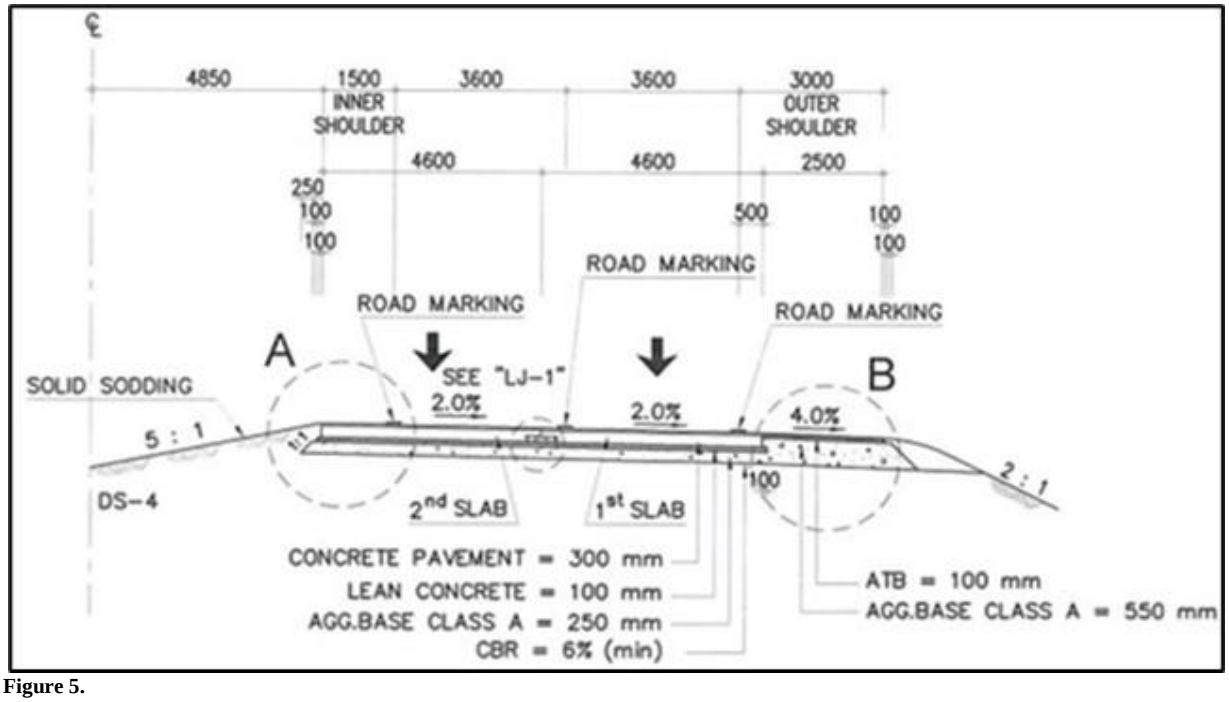

Figure 5.
Typical cross section of concrete pavement.

The testing specifically intended to understand the subbase condition beneath the rigid pavement on a toll road in Indonesia. The initial condition of existing rigid pavement was cracks on whole areas consequently the reconstruction was held. The concrete slab was crushed by breaker; debris was removed then soil sampling was able to be carried out. The concrete slab was reconstructed at the 1st lane of the traffic lane while 2nd traffic lane was still active. Figure 6 depicts a definite slab in Sta. 178 where field study was taking place.

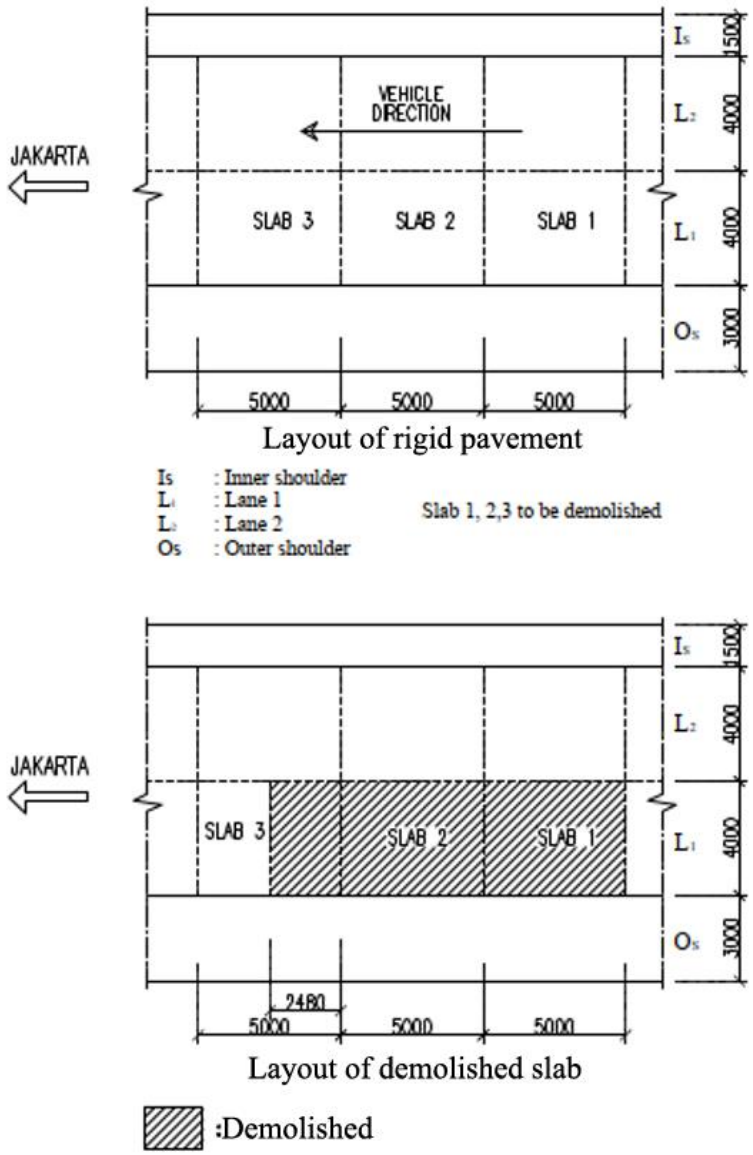

Figure 6.
Location of field study.

Undisturbed samples (UDS) were distributed evenly with total samples of 20 (Figure 7). The samples were taken by using hand auger apparatus then sent to laboratory in paraffin sealed tubes (see Figure 9). The length of the tubes is 60 cm.

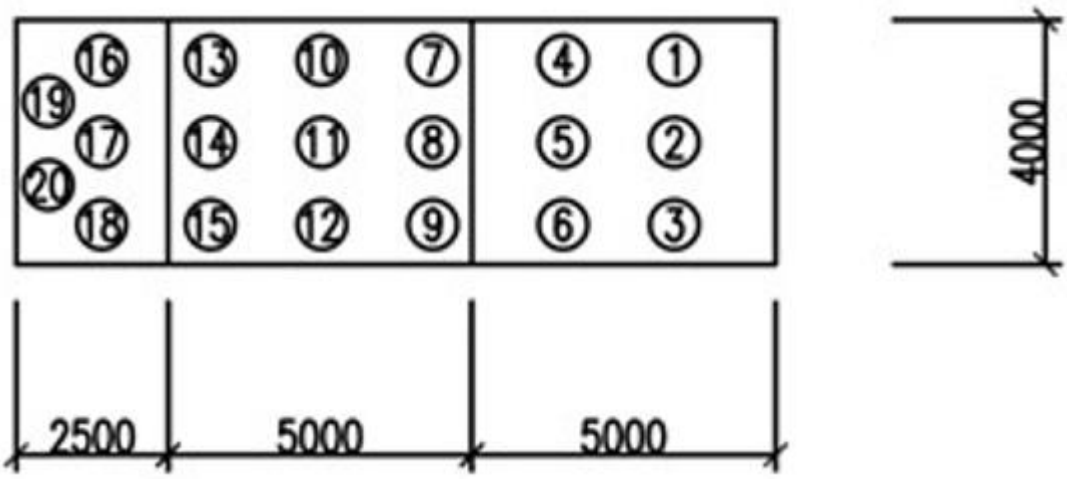

Figure 7.
Undisturbed soil sampling (UDS) point of sampling.

Photos during the test are presented in Figure 8.

Figure **8.**
UDS sampling using hand auger.

Figure 9.
UDS in sealed tubing.

3.4. Properties of Soil

The results of testing in the soil mechanics laboratory yielded soil properties in the form of index properties and mechanical properties. In addition, a conclusion was obtained regarding the type of soil for the layer beneath the rigid pavement.

Soil samples tested in laboratory also showed the characteristics of soil which indicated by index and engineering properties. Index properties include grain size, relative density, Atterberg limits and consistency. Engineering properties consisted of cohesion, internal friction angle, permeability, elasticity, compressibility. Another important result was soil classification which guided by above properties.

Laboratory tests provided result that particle size distribution as listed on Table 4 and Atterberg limit. Plasticity index (IP) ranges from 24.49 – 44.84%. By implementing Unified Soil Classification System (USCS), it was shown that the soil types are silts and clays. It comprises MH (inorganic silts), CH (inorganic clays of high plasticity) and OH (organic clays of medium to high plasticity). While AASHTO soil classification showed, soil classification is silt clayey with liquid limit above 40%.

Table 4.
Soil Classification.

ID	Particle Size Distribution					Atterberg Limits			USCS Classification	AASHTO Classification
	Gravel (%)	Sand (%)	Silt (%)	Clay (%)	Fines (%)	LL (%)	PL (%)	IP (%)		
BH-01	3.94	17.357	38.99	39.51	78.50	72.97	40.96	32.02	MH or OH	A – 7 – 5
BH-02	4.82	17.00	51.15	27.04	78.19	76.52	41.14	35.38	MH or OH	A – 7 – 5
BH-03	3.94	16.57	39.48	40.01	79.50	73.12	38.22	34.90	MH or OH	A – 7 – 5
BH-04	1.96	18.27	46.08	33.69	79.77	77.50	37.65	39.85	MH or OH	A – 7 – 5
BH-05	3.39	18.87	43.30	34.45	77.75	77.09	43.78	33.31	MH or OH	A – 7 – 5
BH-06	2.46	16.28	40.42	40.85	81.27	77.93	40.68	37.25	MH or OH	A – 7 – 5
BH-07	2.67	15.45	55.52	26.36	81.89	78.32	42.71	35.61	MH or OH	A – 7 – 5
BH-08	1.61	11.74	37.88	48.78	86.66	77.40	41.53	35.87	MH or OH	A – 7 – 5
BH-09	4.90	18.47	39.47	27.17	76.64	74.90	35.34	39.56	MH or OH	A – 7 – 5
BH-10	3.35	15.78	38.44	42.44	80.89	80.62	31.96	48.66	CH	A – 7 – 5
BH-11	3.47	18.04	45.16	33.34	78.50	68.91	35.70	33.21	MH or OH	A – 7 – 5
BH-12	14.87	19.88	42.01	23.24	65.25	55.78	29.43	26.35	MH or OH	A – 7 – 5
BH-13	2.54	20.48	47.53	29.45	76.98	68.52	37.94	30.58	MH or OH	A – 7 – 5
BH-14	2.15	16.79	45.58	35.48	81.06	73.09	34.65	38.44	CH	A – 7 – 5
BH-15	2.43	20.41	42.12	35.04	77.16	74.54	37.24	37.30	MH or OH	A – 7 – 5
BH-16	2.43	20.41	42.12	35.04	77.16	74.54	37.24	37.30	MH or OH	A – 7 – 6
BH-17	1.82	19.08	43.19	35.91	79.10	74.13	35.47	38.66	CH	A – 7 – 6
BH-18	3.68	20.69	42.38	33.25	75.63	71.17	35.84	35.33	CH	A – 7 – 6
BH-19	2.63	17.73	44.02	35.62	79.64	76.02	35.87	40.15	CH	A – 7 – 6
BH-20	1.74	18.14	42.68	37.44	80.12	74.12	36.19	37.93	MH or OH	A – 7 – 5

Note: LL : liquid limit
PL : plastic limit
IP : index of plasticity.

Laboratory tests provided result that specific gravity (G_s) of soil ranges from 2.555 - 2.679 ton/m^3, while density (g_{wet}) ranges from 1.64 – 1.78 (t/m^3). Porosity value (e) shows range 1.00 – 1.33 (Table 5).

Table 5.
Soil Index Properties.

ID	WN (%)	γ_{wet} (t/m³)	γ_{dry} (t/m³)	Gs (t/m³)	e	N	S (%)
BH-01	47.04	1.71	1.16	2.610	1.25	0.56	98.40
BH-02	46.17	1.71	1.17	2.650	1.27	0.56	96.23
BH-03	42.60	1.74	1.22	2.640	1.16	0.54	96.79
BH-04	45.03	1.74	1.20	2.622	1.19	0.54	99.25
BH-05	45.23	1.72	1.19	2.595	1.19	0.54	98.89
BH-06	45.59	1.64	1.13	2.630	1.33	0.57	89.92
BH-07	41.37	1.71	1.21	2.631	1.17	0.54	92.64
BH-08	43.66	1.65	1.15	2.623	1.28	0.56	89.54
BH-09	43.58	1.71	1.19	2.572	1.16	0.54	96.52
BH-10	44.32	1.72	1.19	2.614	1.19	0.54	97.15
BH-11	43.78	1.72	1.20	2.649	1.21	0.55	95.92
BH-12	42.51	1.76	1.24	2.664	1.15	0.54	98.12
BH-13	41.71	1.76	1.24	2.634	1.12	0.53	97.91
BH-14	39.94	1.78	1.27	2.620	1.06	0.52	98.50
BH-15	43.44	1.76	1.22	2.691	1.20	0.55	97.56
BH-16	41.39	1.77	1.25	2.679	1.15	0.53	96.79
BH-17	40.37	1.75	1.24	2.586	1.08	0.52	96.75
BH-18	37.70	1.78	1.30	2.597	1.00	0.50	97.43
BH-19	41.94	1.74	1.22	2.555	1.09	0.52	98.39
BH-20	40.28	1.77	1.26	2.651	1.10	0.52	96.89

Note: W_N : Water content.
g_{wet} : Specific gravity of soil in a saturated condition.
g_{dry} : Specific gravity of soil in a dry condition.
n : Porosity.
e : Void ratio.

Laboratory tests also provided result of triaxial and consolidation as presented in Table 6.

Table 6.
Soil Triaxial and Consolidation.

ID	Triaxial		Consolidation			
	c (kg/cm²)	f (º)	e_0 (t/m³)	Pc (kg/cm²)	Cc	Cr
BH-01	0.89	5.14	1.369	0.95	0.368	0.009
BH-02	0.86	5.33	1.281	1.00	0.317	0.017
BH-03	0.88	5.21	1.252	0.97	0.322	0.003
BH-04	0.72	2.10	1.292	1.26	0.395	0.007
BH-05	0.70	2.23	1.498	1.01	0.634	0.019
BH-06	0.68	2.35	1.264	1.00	0.334	0.006
BH-07	0.68	2.42	1.447	0.90	0.412	0.009
BH-08	0.88	5.21	1.525	1.01	0.608	0.035
BH-09	0.86	5.33	1.283	1.01	0.308	0.026
BH-10	0.53	3.07	1.299	0.97	0.309	0.009
BH-11	0.35	3.34	1.259	0.98	0.333	0.004
BH-12	0.25	5.21	1.198	0.95	0.310	0.008
BH-13	0.72	2.10	1.450	0.90	0.410	0.012
BH-14	0.62	3.50	1.304	0.97	0.304	0.010
BH-15	0.49	3.56	1.327	0.99	0.441	0.011
BH-16	0.46	3.75	0.891	0.95	0.224	0.011
BH-17	0.43	3.94	1.295	0.99	0.321	0.013
BH-18	0.35	4.45	1.500	1.01	0.632	0.021
BH-19	0.53	3.09	1.250	0.93	0.315	0.011
BH-20	0.48	3.40	1.195	1.03	0.302	0.012

Note: c : cohesion.
f : internal shear angle.
C_c : compression index.
C_r : re-compression index.
e_0: : initial void ratio.
p_c : pre-consolidation stress.

4. Results and Discussions

This section explains analysis, result and discussion.

4.1. Shear Modulus of Soil Through the Marcuson and Wahls Equation

The soil shear modulus equation according to Marcuson & Wahls is written in Equation 8.

$$G_{max} = \frac{445.(4.4-e)^2}{1+e}(\sigma'_0)^{0.5} \quad (8)$$

By substituting the porosity parameter (e) and the mean effective principal stress (s'_0) in Equation 8, G_{max} is obtained as described in Table 7.

Table 7.
Calculation of Gmax based on the Marcuson & Wahls equation.

ID	E	σ_1	σ_3	$\sigma_0 = (\sigma_1 + \sigma_3)/2$	Gmax (psi)	Gmax (MPa)
BH-01	1.25	1.0000	3.092	2.046	2807.058	28.071
BH-02	1.27	1.0000	3.093	2.046	2747.107	27.471
BH-03	1.16	1.0000	3.083	2.042	3090.089	30.901
BH-04	1.19	1.0000	2.531	1.766	2782.017	27.820
BH-05	1.19	1.0000	2.531	1.766	2782.017	27.820
BH-06	1.33	1.0000	2.497	1.749	2380.201	23.802
BH-07	1.17	1.0000	2.505	1.753	2832.268	28.323
BH-08	1.28	1.0000	3.092	2.046	2717.610	27.176
BH-09	1.16	1.0000	3.092	2.046	3093.493	30.935
BH-10	1.19	1.0000	2.190	1.595	2644.273	26.443
BH-11	1.21	1.0000	1.923	1.462	2477.128	24.771
BH-12	1.15	1.0000	1.082	1.041	2230.559	22.306
BH-13	1.12	1.0000	2.531	1.766	3000.583	30.006
BH-14	1.06	1.0000	2.53	1.765	3201.534	32.015
BH-15	1.20	1.0000	2.15	1.574	2598.601	25.986
BH-16	1.15	1.0000	2.139	1.570	2738.854	27.389
BH-17	1.08	1.0000	2.085	1.543	2928.771	29.288
BH-18	1.00	1.0000	1.921	1.461	3108.412	31.084
BH-19	1.09	1.0000	2.184	1.592	2943.346	29.433
BH-20	1.10	1.0000	2.168	1.584	2904.331	29.043

4.2. Soil Shear Modulus through the Equation by Kakusho et al.

The soil shear modulus equation according to Kakusho et al. is written in Equation 9.

$$G_{max} = \frac{90.(7.32-e)^2}{1+e}(\sigma'_0)^{0.6} \quad (9)$$

By substituting the porosity parameter (e) and the mean effective principal stress (s'_0) into Equation 9, G_{max} is obtained as described in Table 8.

Table 8.
Calculation of Gmax based on the Kakusho equation.

ID	E	σ_1	σ_3	$\sigma_0 = (\sigma_1 + \sigma_3)/2$	Gmax (psi)	Gmax (MPa)
BH-01	1.25	1.0000	3.092	2.046	2264.544	22.645
BH-02	1.27	1.0000	3.093	2.046	2229.825	22.298
BH-03	1.16	1.0000	3.083	2.042	2426.162	24.262
BH-04	1.19	1.0000	2.531	1.766	2171.901	21.719
BH-05	1.19	1.0000	2.531	1.766	2171.901	21.719
BH-06	1.33	1.0000	2.497	1.749	1937.937	19.379
BH-07	1.17	1.0000	2.505	1.753	2196.483	21.965
BH-08	1.28	1.0000	3.092	2.046	2212.712	22.127
BH-09	1.16	1.0000	3.092	2.046	2429.369	24.294
BH-10	1.19	1.0000	2.190	1.595	2043.505	20.435
BH-11	1.21	1.0000	1.923	1.462	1909.026	19.090
BH-12	1.15	1.0000	1.082	1.041	1632.469	16.325
BH-13	1.12	1.0000	2.531	1.766	2295.148	22.951
BH-14	1.06	1.0000	2.53	1.765	2407.525	24.075
BH-15	1.20	1.0000	2.15	1.574	2011.525	20.115
BH-16	1.15	1.0000	2.139	1.570	2088.484	20.885
BH-17	1.08	1.0000	2.085	1.543	2185.161	21.852
BH-18	1.00	1.0000	1.921	1.461	2256.044	22.560
BH-19	1.09	1.0000	2.184	1.592	2209.216	22.092
BH-20	1.10	1.0000	2.168	1.584	2185.028	21.850

4.3. Soil Shear Modulus Through the Hardin and Black Equation

The soil shear modulus equation as suggested by Hardin & Black is written in Equation 10.

$$G_{max} = \frac{1230.(2.973 - e)^2 OCR^k}{1 + e}\sqrt{\sigma'_0} \quad (10)$$

Hardin & Black required the parameters porosity (e), OCR, and k to obtain the G_{max} result, as shown in Table 9.

Table 9.
Calculation of Gmax based on the Hardin & Black equation.

ID	Ip (%)	Φ (°)	Cc/σ'c	OCR	k	e	σ_1	σ_3	$\sigma_0 = (\sigma_1 + \sigma_3)/2$	Gmax (psi)	Gmax (MPa)
BH-01	32.02	5.14	0.228	5.745	0.252	1.25	1.0000	3.092	2.046	3607.310	36.073
BH-02	35.38	5.33	0.241	5.885	0.272	1.27	1.0000	3.093	2.046	3642.021	36.420
BH-03	34.90	5.21	0.239	6.015	0.269	1.16	1.0000	3.083	2.042	4336.551	43.366
BH-04	39.85	2.10	0.257	24.436	0.297	1.19	1.0000	2.531	1.766	6171.042	61.710
BH-05	33.31	2.23	0.233	19.478	0.260	1.19	1.0000	2.531	1.766	5132.146	51.321
BH-06	37.25	2.35	0.248	10.976	0.274	1.33	1.0000	2.497	1.749	4387.253	43.873
BH-07	35.61	2.42	0.242	18.242	0.274	1.17	1.0000	2.505	1.753	5399.733	53.997
BH-08	35.87	5.21	0.243	6.144	0.275	1.28	1.0000	3.092	2.046	3645.344	36.453
BH-09	39.56	3.50	0.256	6.432	0.296	1.16	1.0000	3.092	2.046	4656.547	46.566
BH-10	48.66	3.07	0.290	16.848	0.345	1.19	1.0000	2.190	1.595	6019.119	60.191
BH-11	33.21	5.34	0.233	10.978	0.259	1.21	1.0000	1.923	1.462	3886.526	38.865
BH-12	35.89	5.21	0.242	6.147	0.275	1.15	1.0000	1.082	1.041	3198.259	31.983
BH-13	36.60	2.10	0.245	22.822	0.277	1.12	1.0000	2.531	1.766	6346.734	63.467
BH-14	44.84	3.50	0.276	13.021	0.327	1.06	1.0000	2.53	1.765	6711.215	67.112
BH-15	30.67	3.56	0.223	9.398	0.244	1.20	1.0000	2.15	1.574	3809.284	38.093
BH-16	24.49	3.75	0.201	7.485	0.234	1.15	1.0000	2.139	1.570	3612.072	36.121
BH-17	25.13	3.94	0.203	7.088	0.211	1.08	1.0000	2.085	1.543	3976.746	39.767
BH-18	29.83	4.45	0.220	7.111	0.260	1.00	1.0000	1.921	1.461	4558.365	45.584
BH-19	27.73	3.09	0.213	6.701	0.226	1.09	1.0000	2.184	1.592	4503.635	45.036
BH-20	33.33	3.40	0.233	10.673	0.260	1.10	1.0000	2.168	1.584	4785.964	47.860

4.4. Soil Shear Modulus Through the Menard Equation

Menard defines the shear modulus equation through Equation 11, to obtain the G_{max} result, as shown Table 10.

$$G_{max} = \frac{E}{2(1 + \nu)R_M} \quad (11)$$

Table 10.
Calculations of G_{max} According to Menard equation.

ID	Ip (%)	RM	E	Soil Class	v	Gmax (MPa)
BH-01	32.02	0.241	12.1	MH or OH	0.3	19.336
BH-02	35.38	0.255	11.2	MH or OH	0.3	16.884
BH-03	34.90	0.253	10.3	MH or OH	0.3	15.654
BH-04	39.85	0.274	9.3	MH or OH	0.3	13.038
BH-05	33.31	0.246	9.3	MH or OH	0.3	14.527
BH-06	37.25	0.263	11.2	MH or OH	0.3	16.527
BH-07	35.61	0.256	12.1	MH or OH	0.3	18.170
BH-08	35.87	0.257	14.0	MH or OH	0.3	20.932
BH-09	39.56	0.273	12.1	MH or OH	0.3	17.040
BH-10	48.66	0.312	9.3	CH	0.4	10.637
BH-11	33.21	0.246	14.0	MH or OH	0.3	21.906
BH-12	35.89	0.257	9.3	MH or OH	0.3	13.900
BH-13	36.60	0.260	9.3	MH or OH	0.3	13.737
BH-14	44.84	0.296	11.2	CH	0.4	13.522
BH-15	30.67	0.235	16.8	MH or OH	0.3	27.510
BH-16	24.49	0.208	18.7	MH or OH	0.3	34.527
BH-17	25.13	0.211	15.9	CH	0.4	26.905
BH-18	29.83	0.231	12.1	CH	0.4	18.968
BH-19	27.73	0.222	16.8	CH	0.4	26.998
BH-20	33.33	0.246	18.7	MH or OH	0.3	29.199

4.5. Analysis of Calculated G_{max}

Now four G_{max} values are obtained as result of applying four empirical equations and utilizing laboratory test data as well as references. The four G_{max} values are summarized in Table 11 (unit MPa).

Table 11.
Summary of G_{max}.

Equation	Marcuson & Wahls	Kakusho	Hardin & Black	Menard
G_{max} maximum	32.015	24.294	67.112	34.527
G_{max} minimum	22.306	16.325	31.982	10.634
G_{max} average	28.004	21.632	46.192	19.474

The summary of G_{max} is compared in chart form through Figure 10 presented below.

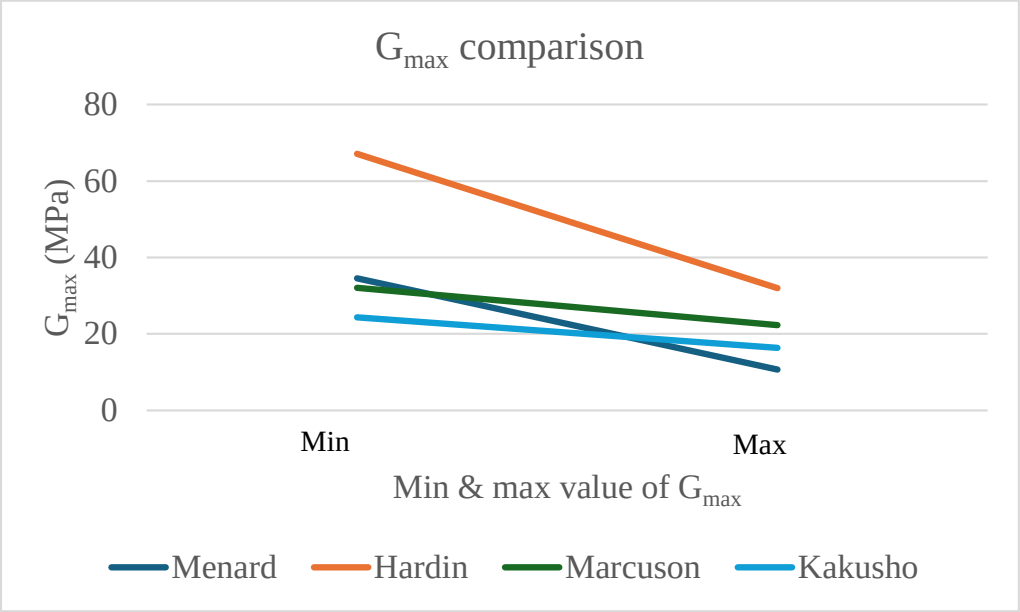

Figure 10.
G_{max} comparison.

In Figure 10, the G_{max} value from the Hardin & Black equation is above the G_{max} values from the other equations, while the G_{max} values from the Marcuson, Menard, and Kakusho equations fall within a corridor of closely spaced maximum and minimum values.

Next, all G_{max} results (BH1–BH20) are plotted in a diagram against Ip, from which a regression equation can be obtained showing the relationship between G_{max} and Ip.

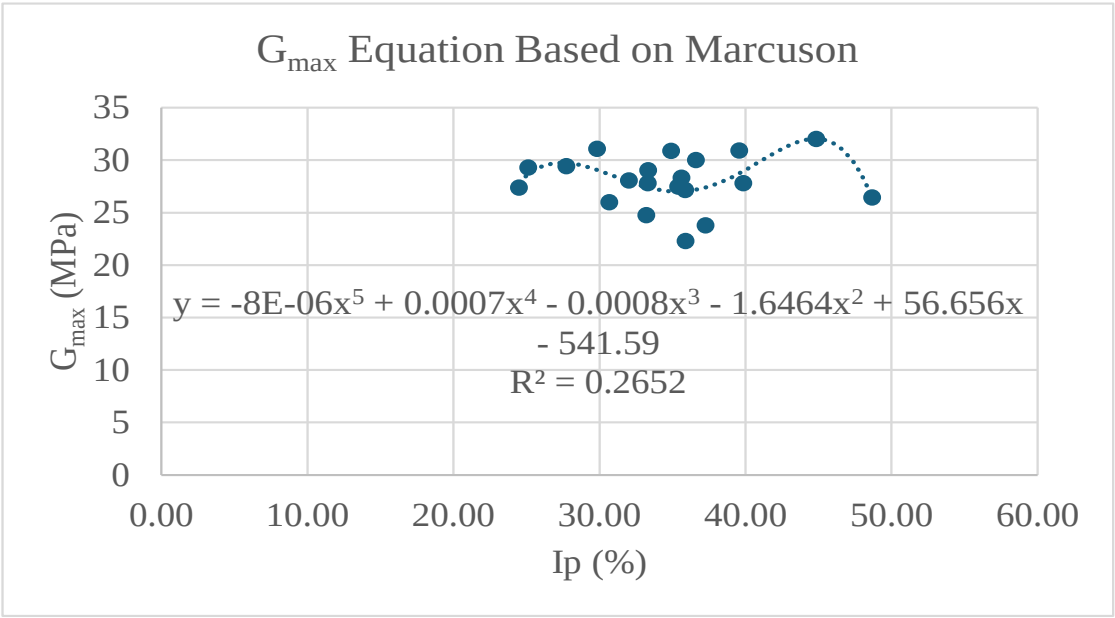

Figure 11.
Marcuson G_{max} plotting & equation.

Figure 11 is the plot and regression equation based on Marcuson. The correlation is not sufficiently good, as evidenced by $R^2 = 0.2652$.

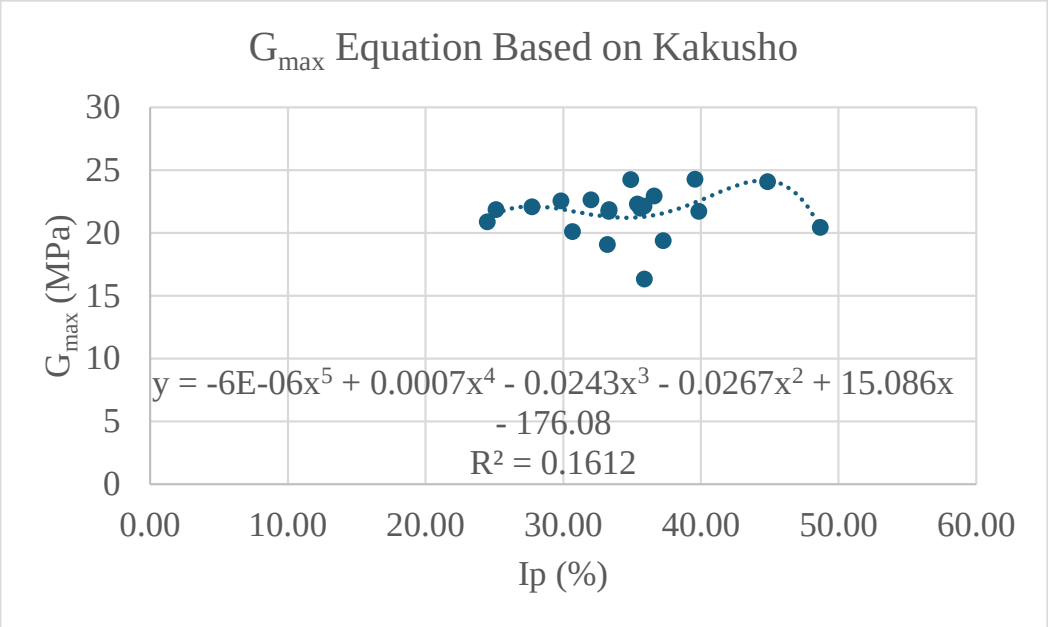

Figure 12.
Kakusho G_{max} plotting & equation.

Figure 12 is the plot and regression equation based on Kakusho. Although a 5th-order polynomial equation has been used, it is concluded that the correlation is not sufficiently good, as evidenced by $R^2 = 0.1612$.

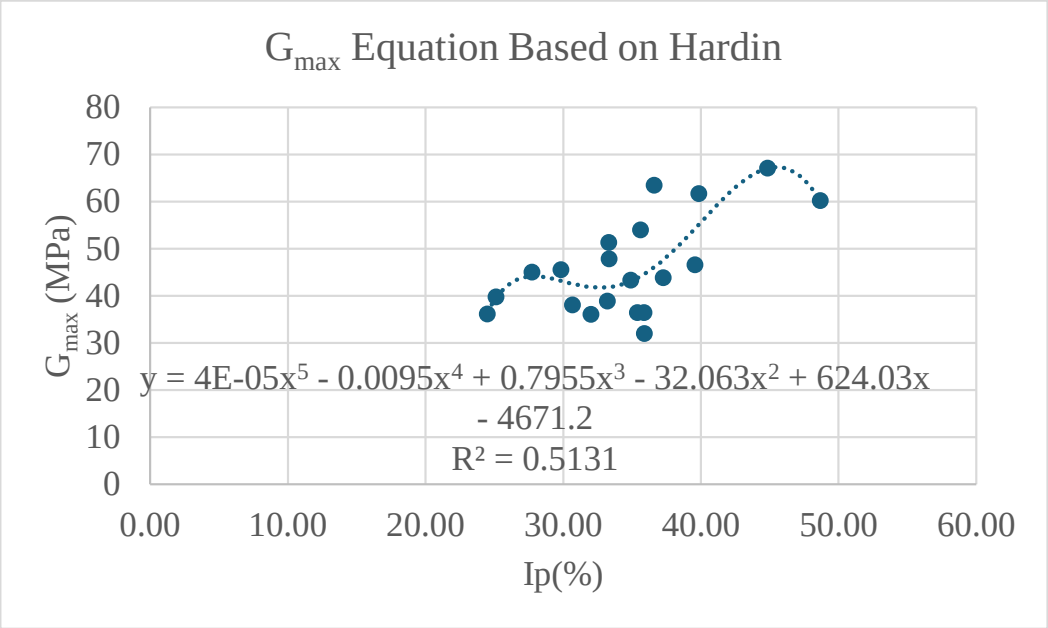

Figure 13.
Hardin & Black G_{max} plotting & equation.

Figure 13 is the plot and regression equation based on the research of Hardin & Black. Using a 5th-order polynomial equation, a good correlation can be seen, indicated by $R^2 = 0.5131$.

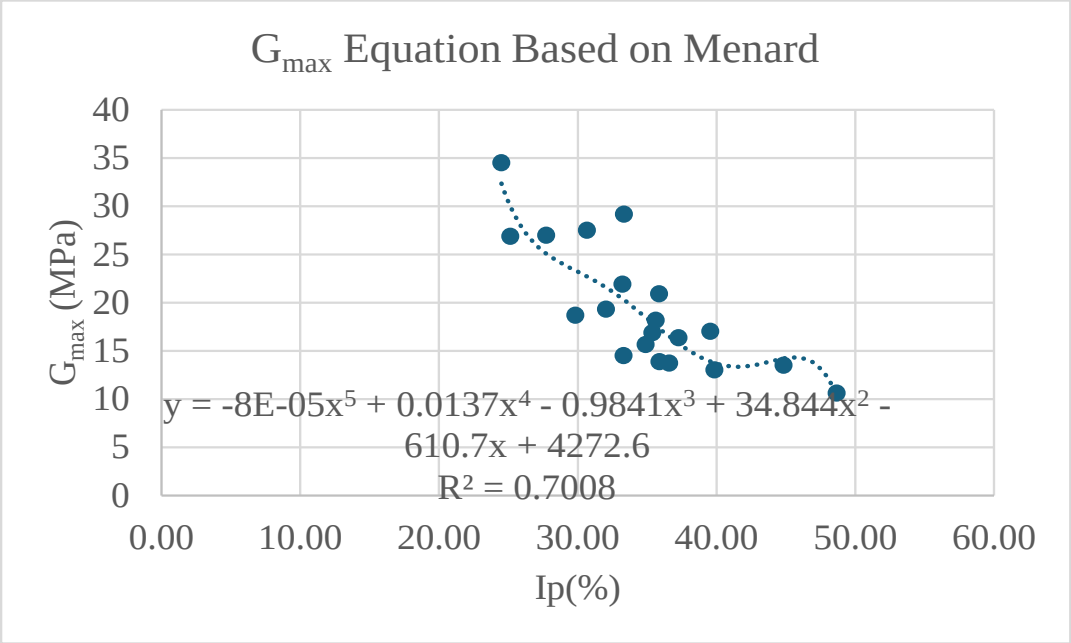

Figure 14.
Menard G_{max} plotting & equation.

Figure 14 is the plot and regression equation based on Menard. Using a 5th-order polynomial equation, a fairly good correlation is observed, indicated by $R^2 = 0.7008$.

4.6. Proposed equation of G_{max}

From the calculations in Section 4.5, there are four regression equations representing the correlation between Ip and G_{max}. The four equations along with their correlation strengths are summarized in Table 12.

Table 12.
Summary of regression equation G_{max}.

Creator	Equation	R^2	Justification
Marcuson	G_{max} = -8E-06(Ip)^5 + 0.0007(Ip)^4 - 0.0008(Ip)^3 - 1.6464(Ip)^2 + 56.656(Ip) - 541.59	0.2652	Not accepted
Kakusho	G_{max} = -6E-06(Ip)^5 + 0.0007(Ip)^4 - 0.0243(Ip)^3 - 0.0267(Ip)^2 + 15.086Ip - 176.08	0.1612	Not accepted
Hardin	G_{max}= 4E-05(Ip)^5 - 0.0095(Ip)^4 + 0.7955(Ip)^3 - 32.063(Ip)^2 + 624.03(Ip) - 4671.2	0.5131	Accepted
Menard	G_{max} = -8E-05(Ip)^5 + 0.0137(Ip)^4 - 0.9841(Ip)^3 + 34.844(Ip)^2 - 610.7Ip + 4272.6	0.7008	Accepted

In Table 12 above, it is concluded that the regression based on the Menard equation has the highest correlation between G_{max} and Ip, with $R^2 = 0.7008$. This can be understood since the Menard equation indirectly accounts for the Ip factor through the R_M variable. Similarly, the regression equation based on Hardin & Black has a good correlation (R^2 = 0.5131), as the Ip factor is accommodated through the k variable (see Section 3.1).

Thus, this study proposes Equation 12 as the proposed equation for the relationship between G_{max} and Ip (units in MPa).

$$G_{max} = -8E\text{-}05(Ip)^5 + 0.0137(Ip)^4 - 0.9841(Ip)^3 + 34.844(Ip)^2 - 610.7Ip + 4272.6 \quad (12)$$

To simplify the formula and its usage, Equation 13 can be reduced to a 2nd-order polynomial with R^2 of 0.687, as follows.

$$G_{max} = 0.0313(Ip)^2 - 3.1147Ip + 88.798 \quad (13)$$

5. Conclusion

This study shows that calculating the soil shear modulus using in-situ soil data beneath rigid toll road pavements provides adequate results and is feasible for use in the dynamic analysis of rigid pavement slabs.

G_{max} from Marcuson, Kakusho and Menard equations produced maximum and minimum values within similar corridors. While G_{max} came from Hardin tends to be higher than Marcuson, Kakusho and Menard.

The calculation of soil shear modulus (G_{max}) is made possible based on primary data of Plasticity Index (Ip) using a semi-empirical equation:

$$G_{max} = -8E\text{-}05(Ip)^5 + 0.0137(Ip)^4 - 0.9841(Ip)^3 + 34.844(Ip)^2 - 610.7Ip + 4272.6 \quad (12)$$

While simple equation is required, G_{max} semi-empirical equation can be utilized :

$$G_{max} = 0.0313(Ip)^2 - 3.1147Ip + 88.798 \quad (13)$$

The implementing those results, designing a rigid pavement slab may be used above G_{max} values and equations to carry dynamic analysis design.

References

[1] Y. Balekar and M. Irshad, "Effect of dynamic load on rigid pavement," *International Journal of Engineering Research & Technology*, vol. 4, no. 3, 2015.

[2] M. F. Darestani, D. P. Thambiratnam, D. Baweja, and A. Nataatmadja, "Dynamic response of concrete pavements under vehicular loads," in *In Scientific Committee, IABSE (Ed.), Proceedings of the IABSE Symposium: Response to tomorrow's challenges in structural engineering*, Budapest, Hungary, 2006. https://doi.org/10.2749/222137806796169164

[3] V. Sawant, "Dynamic analysis of rigid pavement with vehicle–pavement interaction," *International Journal of Pavement Engineering*, vol. 10, no. 1, pp. 63-72, 2009. https://doi.org/10.1080/10298430802342716

[4] W. Alisjahbana and S. Wangsadinata, "Dynamic of rigid pavement," in *Proceedings of the Ninth Asia–Pacific Conference on Structural Engineering and Construction*, 2003.

[5] S. O. Rahman and I. Anam, "Dynamic analysis of concrete pavement under moving loads," *Journal of Civil and Environmental Engineering*, vol. 1, no. 1, pp. 1-6, 2005.

[6] T. P. Nguyen, D. T. Pham, and P. H. Hoang, "A new foundation model for dynamic analysis of beams on nonlinear foundation subjected to a moving mass," *Procedia Engineering*, vol. 142, pp. 166-173, 2016. https://doi.org/10.1016/j.proeng.2016.02.028

[7] S. W. Alisjahbana, I. Alisjahabana, S. Kiryu, and B. S. Gan, "Semi analytical solution of a rigid pavement under a moving load on a Kerr foundation model," *Journal of Vibroengineering*, vol. 20, no. 5, pp. 2165-2174, 2018. https://doi.org/10.21595/jve.2018.20082

[8] A. Das, *Analysis of pavement structures*. Boca Raton, FL: CRC Press, 2015.

[9] B. O. Hardin and V. P. Drnevich, "Shear modulus and damping in soils: Design equations and curves," *Journal of the Soil Mechanics and Foundations Division*, vol. 98, no. 7, pp. 667-692, 1972. https://doi.org/10.1061/JSFEAQ.0001760

[10] T. Iwasaki, F. Tatsuoka, and Y. Takagi, "Shear moduli of sands under cyclic torsional shear loading," *Soils and Foundations*, vol. 18, no. 1, pp. 39-56, 1978. https://doi.org/10.3208/sandf1972.18.39

[11] K. Gabryś and A. Szymański, "The evaluation of the initial shear modulus of selected cohesive soils," *Studia Geotechnica et Mechanica*, vol. 37, no. 2, pp. 3-9, 2015. https://doi.org/10.1515/sgem-2015-0014

[12] H. W. Nasarani, A. Rifaâ, and H. C. Hardyatmo, "The effect of adding volcanic ash to soft soil on the maximum shear modulus based on UU triaxial testing," *Global Tech Journal*, vol. 8, no. 1, 2019.

[13] E. Purwanto, *Nilai modulus geser tanah berdasarkan rumus Hardin & Drnevich (1972) dan Menard (1965)*. Surakarta, Indonesia: Civil Communication Media, 1972.

[14] ASTM International, *Standard test method for consolidated undrained triaxial compression test for cohesive soils (ASTM D4767–11, Reapproved 2020)*. West Conshohocken, PA: ASTM International, 2020.

[15] P. W. Mayne, "Determining OCR in clays from laboratory strength," *Journal of Geotechnical Engineering*, vol. 114, no. 1, pp. 76-92, 1988. https://doi.org/10.1061/(ASCE)0733-9410(1988)114:1(76)

[16] J. K. H. Wong, S. Y. Wong, and K. Y. Wong, "Extended model of shear modulus reduction for cohesive soils," *Acta Geotechnica*, vol. 17, no. 6, pp. 2347-2363, 2022. https://doi.org/10.1007/s11440-021-01398-0

[17] Zsolt Szilvágyi1, Péter Hudacsek1, and R. P. Ray., "Soil shear modulus from resonant column, torsional shear, and bender element tests," *International Journal of GEOMATE*, vol. 10, no. 2, 2016.

[18] Q. Zhai *et al.*, "A new mathematical model for the estimation of shear modulus for unsaturated compacted soils," *Canadian Geotechnical Journal*, vol. 61, no. 10, pp. 2124-2137, 2024. https://doi.org/10.1139/cgj-2023-0409

[19] J. E. Bowles, *Foundation analysis and design*, 5th ed. New York: The McGraw-Hill Companies, Inc., 1997.

[20] W. F. Marcuson and H. E. Wahls, "Effects of time on damping ratio of clays," *Dynamic Geotechnical Testing*, vol. 654, pp. 126-147, 1978.

[21] O. Kakusho and M. Yanagida, "Hierarchical AR model for time varying speech signals," in *ICASSP '82. IEEE International Conference on Acoustics, Speech, and Signal Processing*, 1982. https://doi.org/10.1109/ICASSP.1982.1171643

[22] H. Menard, "The world-wide oceanic rise-ridge system," *Philosophical Transactions of the Royal Society of London. Series A, Mathematical and Physical Sciences*, vol. 258, no. 1088, pp. 109-122, 1965. https://doi.org/10.1098/rsta.1965.0026

[23] D. Urbaitis, I. Lekstutyte, and D. Gribulis, "Overconsolidation ratio determination of cohesive soil," in *Proceedings of the 13th Baltic Sea Geotechnical Conference. Lithuanian Geotechnical Society, Lithuania*, 2016.